



Computational Fluid Dynamics validation study of an axial flow impeller often used in Anaerobic Digesters

D. Fernandes del Pozo*, A. Liné**, J. Dedeyne***, K. M. Van Geem***, I. Nopens*

*BIOMATH, Department of Data Analysis and Mathematical Modelling, Ghent University, Coupure Links 653, B-9000, Ghent, Belgium. david.fernandesdelpozo@ugent.be, ingmar.nopens@ugent.be

**LISBP, Université de Toulouse, INSA, INRA, CNRS, Toulouse, France. alain.line@insa-toulouse.fr

*** Laboratory for Chemical Technology, Technologiepark 914, B-9052, Ghent University, Ghent, Belgium, jensn.dedeyne@ugent.be, kevin.vangeem@ugent.be

Abstract: This work presents a detailed validation study to build a Computational Fluid Dynamics (CFD) model for mechanically mixed anaerobic digesters using OpenFOAM®. The methodology analyses the impact of different CFD settings (in terms of geometry, mesh, numerics, and transport models) with two validation test cases using water and a non-Newtonian fluid when a standard hydrofoil impeller is used. The results show that the evaluation of different settings is crucial for the development of accurate and reliable models for anaerobic digesters by identifying the source of its modelling errors. More specifically, the calibration of the rheological model for anaerobic digesters is shown to be especially important when determining even the velocity fields.

Keywords: Mechanical mixer; A310; rheology; CFD methodology; validation; OpenFOAM.

Introduction

With newer and stricter environmental regulations, Waste Water Treatment Plants (WWTPs) are under constant pressure to minimise energy consumption while providing an adequate mixing level for their energy intensive mixing operations. In these facilities, anaerobic digesters are usually designed to be completely mixed by mechanical stirrers, being an energy intensive operations. In this respect, full-scale mechanical mixers can benefit from Computational Fluid Dynamics (CFD) by exploring different mixing for energy optimisation. However, the lack of validation studies on CFD of mechanical mixers for anaerobic digesters might explain the large uncertainties associated with these models, and therefore the lack of a general and detailed CFD methodology. The evaluation and quantification of the influence of the different source of modelling uncertainties is crucial for the development of reliable CFD simulations for any scale. This research aims to fill this gap by following the GMP rules of the IWA CFD task group (Wicklein *et al.*, 2015), and to provide results for two validation lab-scale cases for a mechanical stirrer using water and a non-Newtonian fluid (Carbopol, which rheologically mimics the behaviour of digested sludge; Eshtiaghi *et al.*, 2012). More specifically, the methodology applies different CFD model settings in terms of geometry, numerical discretization, and different transport models to evaluate their efficiency. This is an initial important step towards unravelling the true mixing behaviour in anaerobic digesters.

Material and Methods

The OpenFOAM® toolbox v6 is used to run the CFD simulations. Paraview 5.6 and Python's jupyter notebooks have been used for data post-processing and visualisation. The domain of interest is a cylindrical tank ($V=70L$) equipped with four equidistant baffles. The cylindrical tank has a flat bottom equal to tank height ($H=T=0.45m$). The axial impeller is a hydrofoil Lightning A310 ($D=H/3$) mounted at the center, rotating at 200rpm for the water case, and with a bottom clearance ($C=T/3$). The commercial

software PointWise® (PW; PointWise, Inc.) and the open-source SnappyHexMesh (SHM) are used as meshing tools to discretise the domain for the drawn and scanned geometry respectively (see Figure 3). A Temperature of 20°C was selected for water properties ($\rho = 1000\text{kg/m}^3$; $\mu = 10^{-3} \text{ Pa}\cdot\text{s}$) and the $k-\omega$ SST turbulence model was selected for the results shown in the abstract. For the non-Newtonian case (Carbopol, 0.06%), the Herschel-Bulkley rheological model was selected to be equivalent to a medium-high sludge concentration.

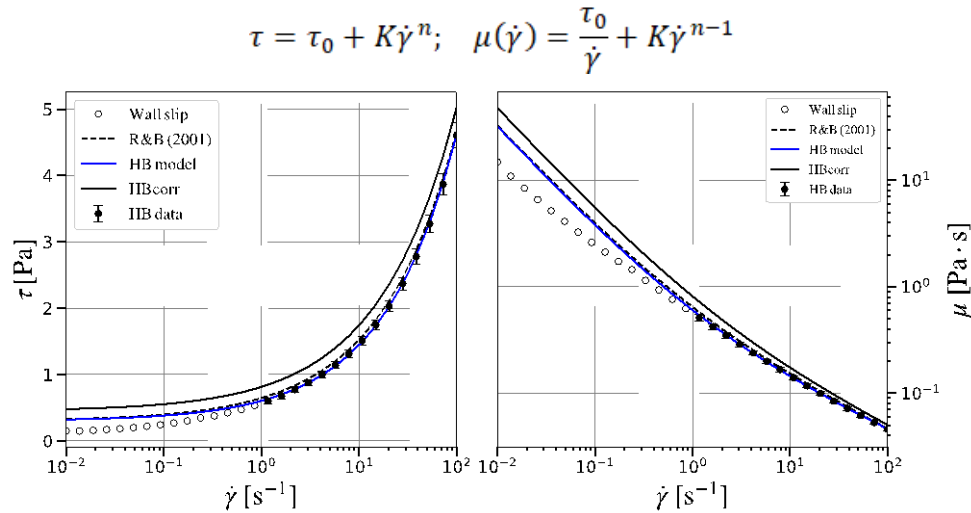


Figure 1: Rheological profiles of Carbopol with a calibrated Herschel-Bulkley model ($\tau_0=0.300$; $K=0.303$; $n=0.577$) and HB parameters from Robert and Barnes (2001; $\tau_0=0.300$; $K=0.345$; $n=0.55$). HB corrected parameters ($\tau_0=0.450$; $K=0.363$; $n=0.55$).

The PIV data (Fernandes del Pozo *et al*, 2019) for the non-Newtonian case was obtained in-house using a PIV software for the geometry described above (DynamicStudio 2015a, Dantec Dynamic, Denmark).

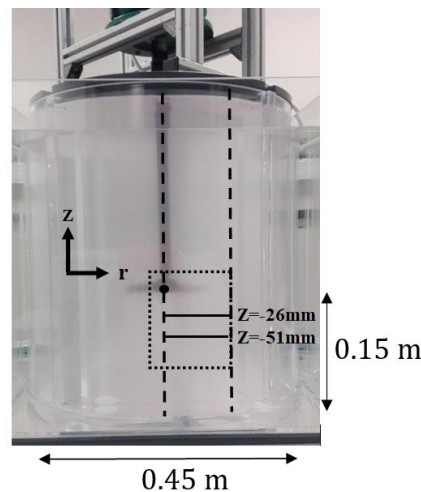


Figure 2 Dimensions of the PIV setup and location of the laser sheet with respect to the impeller. The dashed lines indicates the maximum depth of field imposed by the baffles and the axis of symmetry. The fine dashed line on the left figure indicates an approximate size of the r - Z field. The impeller rotates in the clockwise direction.

Results and Discussion

Fluid: Water

After a mesh independency test, a mesh is obtained which resolves with sufficient accuracy the main properties of interest for the validation study (velocity fields, and the Power consumed by the impeller). Due to the highly complex airfoil shape of the impeller, extra care is taken to ensure that the produced mesh has the desired mesh quality while representing accurately the geometry and providing enough refinement to resolve the flow features. The resulting mesh was ensured to have a maximum non orthogonality and skewness below 72° and 1, respectively. The cell count for the different meshes of figure 5: 3.285.629 cells (R3: draw); 6.454.302 cells (R6: scan and upwind); and 4.181.603 cells (Arbitrary Mesh Interface, AMI). The power numbers obtained by integration of the torque on the impeller surface (sum of pressure and viscous moments) are 0.324 and 0.270, quite close to the reported experimental value of 0.284 (0.8W from Bugay, 2002) for this type of impeller.

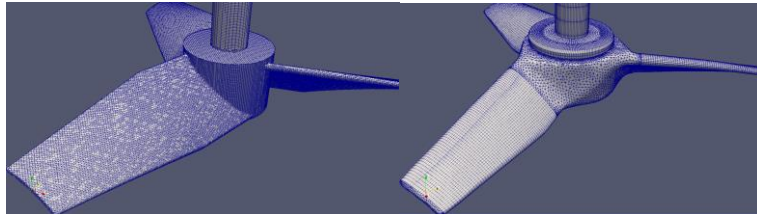


Figure 3 Visualisation example of the surface mesh used for the A310 impeller using an in-house CAD drawing (left, R3, SHM) and the 3D scanned geometry (right, R6,PW).

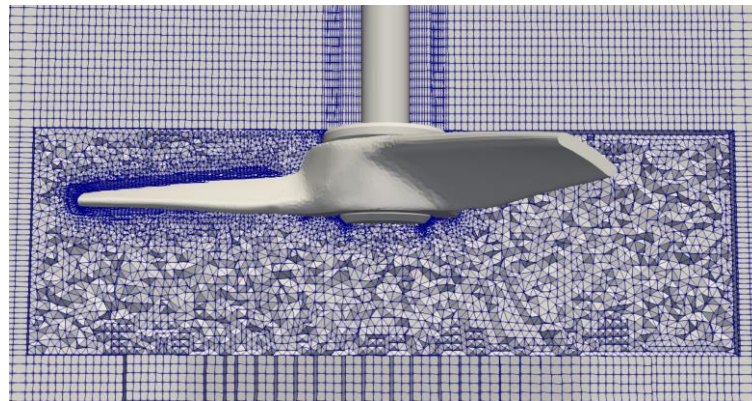


Figure 4 Visualisation example of the mesh around the AMI interfaces and impeller (R4).

The simulation details are contained in Table 1. The settings were adjusted in each case as a compromise between stability and accuracy. It is noted that 2nd order schemes were preferred for all variables, but the presence of limiters was necessary in some cases to avoid divergence.

Table 1 Overview of OpenFOAM settings applied for the water CFD simulations.

Solver	SimpleFoam (Multiple Reference Frame, MRF) pimpleFoam (Sliding Mesh, SM; AMI); $\Delta t=10^{-5}$ s.
Turbulence model	$k-\omega$ SST
Boundary conditions	
Wall treatment for turbulent quantities	Impeller +shaft with no wall functions Standard wall functions at reactor walls
U	Surface (slip) Impeller + MRF/AMI shaft (movingWallVelocity) Shaft (rotatingWallVelocity) Walls + baffles (fixedValue=0)
p	zeroGradient
Discretization schemes	
Gradient	CellLimited leastSquares 0/0.5/1
Divergence	Gauss linearUpwindV grad(U) (Velocity) Gauss upwind/linearUpwind (turbulent quantities)
Laplacian	Gauss linear limited corrected 0.5/1.

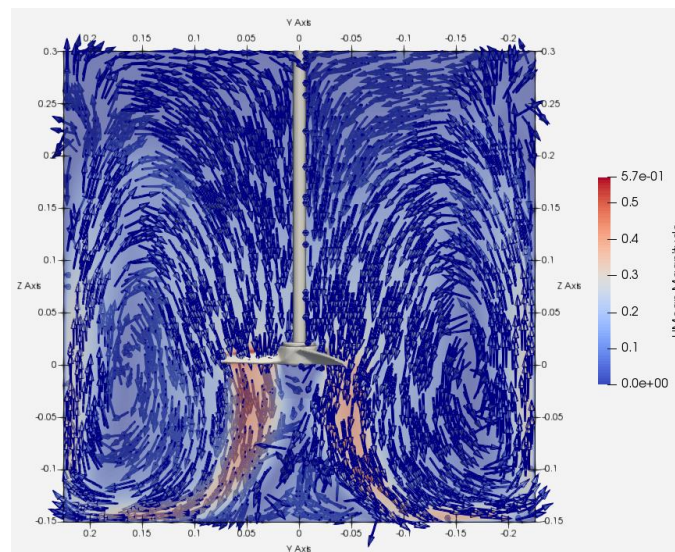


Figure 5 Contour and vector plot of velocity magnitude of an axial-radial plane for the AMI water case (R4 mesh) with the impeller rotating at 200rpm.

In Figure 5, the main flow features can be observed. The development of a downward jet is a flow feature characteristic of axial impellers such as in A310 (Bugay, 2002).

Next, the three component velocity profiles are extracted by averaging over the angular direction the radial profiles at a certain height. This is performed for both cases (U velocity field for MRF and U_{mean} field obtained from *controlDict* functions for the AMI case).

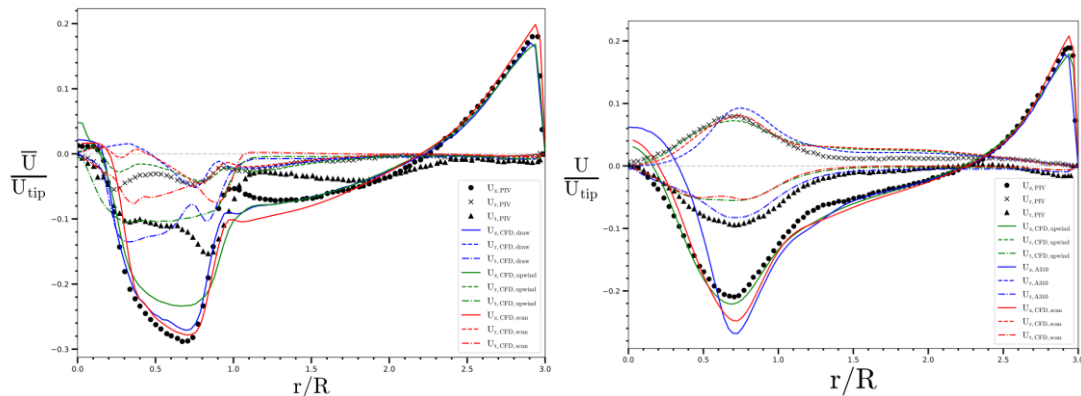


Figure 6 Axial, radial, and tangential velocity radial profiles normalised by the tip impeller speed at $Z=5\text{mm}$ [left] and 85mm [right] below the impeller. The Figure shows the effect of 1) the geometry details of the A310 impeller using an in-house drawing (drawing) and 3D scan version (CFD,scan), and 2) the effect of numerical discretisation on the convective term (First order) with the scanned geometry. Experimental points were taken from Particle Image Velocimetry (PIV) experimental results from Bugay *et al.* (2002). $R=0.075\text{m}$. All simulations were run with the MRF approach.

The results of Figure 6 illustrate the differences when using a different numerical scheme for the convection term (*upwind* vs *LinearUpwind*) and a different geometry. Surprisingly, the results of the drawn geometry are similar to that of the 3D scan even for such a complex geometry, suggesting that they both produce a similar flow field around the impeller (as a result of having a sufficiently refined mesh). It is also clear that the first order schemes provide a decent numerical prediction, although it smooths the profiles due to numerical dissipation. Additionally, deficiencies of the $k-\omega$ SST turbulence model can be observed since it mostly under predicts the tangential and radial components due to an artificial increase in turbulent viscosity (it does not take into account rotational strain history). Lastly, the comparison at different locations ($Z=-5,-85\text{mm}$) ensures that the degree of accuracy of the CFD model remains acceptable in most parts of the tank. These results are in agreement with CFD simulations of Lane (2017).

Fluid: Carbopol

50rpm

In a first stage, the CFD model is compared against PIV data obtained at 50rpm to evaluate the accuracy of the rheological model (only radial and axial components were obtained). At this rotational speed, the fluctuations are small and the flow regime can be considered laminar. Thus, the simulations are run using the MRF approach with a laminar model.

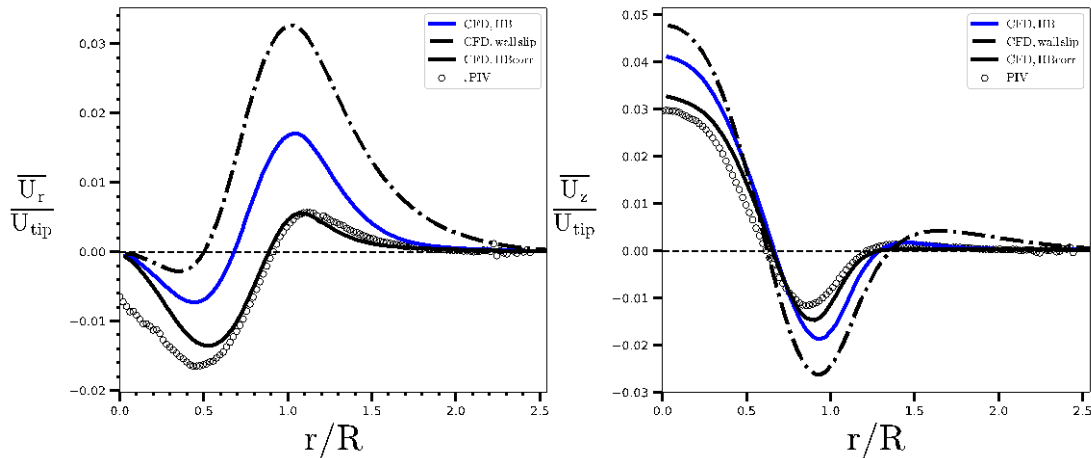


Figure 7 Radial [left] and axial [right] velocity radial profiles normalised by the tip impeller speed at $Z=-26\text{mm}$ below the impeller using different rheological models and rotating at 50rpm. $R=0.075\text{m}$. All simulations were run with the MRF approach.

As it is observed in Figure 7, the HB model with and without wall slip fail to accurately capture the radial and axial components. This is explained by the low yield stress predicted by these models, resulting in a fluid experiencing lower viscosities than it is observed and thereby yielding high velocity profiles. The Herschel-Bulkley correction on yield stress and consistency index offers a more accurate overlap, questioning the obtention of HB parameters from rheometer data even with wall-slip correction. The origin of the HB correction lies on the work of Chambon (2014), where the calibrated parameters obtained from the rheometer data did not match the experimental velocity profiles and adjustments to the original parameters need to be made. However, the origin of this discrepancy remains unclear, and additional viscoelastic properties might be necessary to better describe Carbopol properties.

250rpm

After an extensive evaluation of the accuracy of the different components of the CFD model for water and Carbopol, the accuracy of the CFD model is evaluated for a rotational speed of 250rpm, involving a transitional flow regime and the results can be seen Figure 8:

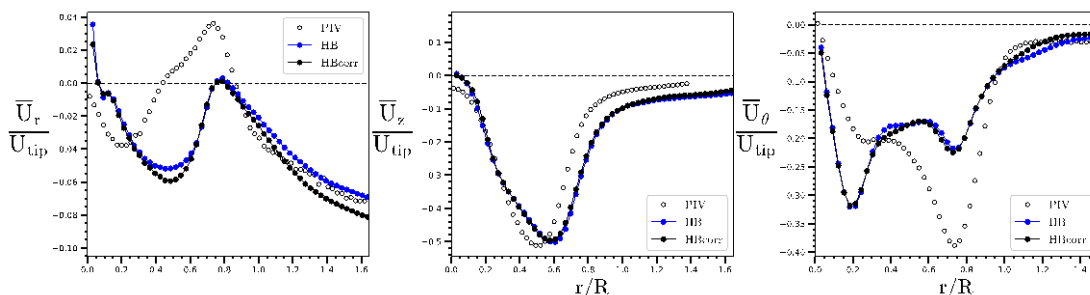


Figure 8 Radial [left] and axial [middle] and tangential [right] velocity radial profiles normalised by the tip impeller speed at $Z=-26\text{mm}$ below the impeller using different rheological models and rotating at 250rpm. $R=0.075\text{m}$. All simulations were run with the MRF approach.

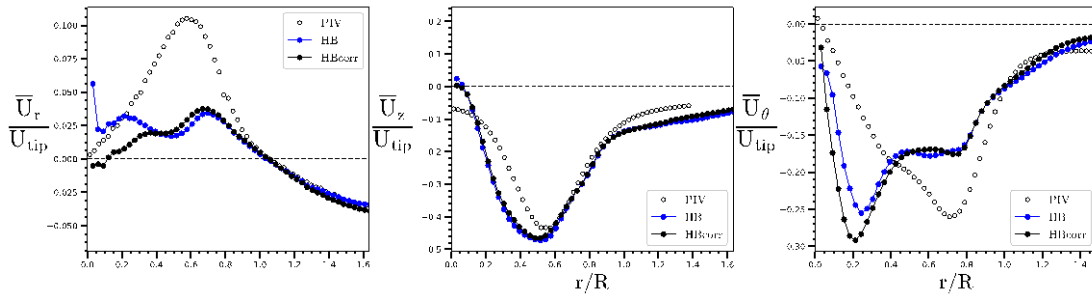


Figure 9 Radial [left] and axial [middle] and tangential [right] velocity radial profiles normalised by the tip impeller speed at $Z=-51\text{mm}$ below the impeller using different rheological models and rotating at 250rpm . $R=0.075\text{m}$. All simulations were run with the MRF approach.

It is possible to observe that the CFD model gives an overall fair prediction of the order of magnitude for the three velocity component profiles for Figures 7 and 8. However, it is noted that the radial component is not well captured by the CFD model and the tangential CFD component fails to predict the intensity of the largest peak. The origin of such discrepancies can be related with: 1) an incorrect description of the correct rheological behaviour at such high shear rates, 2) the already described pitfalls of the $k-\omega$ SST turbulence model predicting the tangential components in swirly flow, and 3) the interaction of all numerical components in the CFD model. The latter ones are believed to be minimised as demonstrated in the validation exercise with the water case. Additionally, it is known in literature that the correct description of the main flow features arising in transitional flow are hard to capture. This might suggest that more complex and computationally intensive CFD approaches should be taken if a higher accuracy is desired (e.g. MRF vs AMI, or Large Eddy Simulation, LES). It is also noted that even when the HB model was modified to improve the rheological behaviour at high viscosities (low shear rates), the prediction of lower viscosities is mainly affected by the consistency index and power index alone (as the correction was mainly applied to the yield stress). This is observed by the small difference between both rheological models tested at 250rpm .

Conclusions

This research shows the methodology followed to build a mechanically mixed CFD model and studied the influence of different CFD settings to represent accurately the main relevant hydrodynamic fields. The performance of the CFD model at different locations below the impeller was possible since a high-quality data set was obtained to make such analysis. The results indicated that for non-Newtonian flows in stirring tanks, it is still challenging to correctly capture radial and tangential components for such complex 3D flows at the rotational speeds considered. The results also show the great influence of the non-Newtonian behaviour on the hydrodynamic fields compared to the results when water is used as a fluid. The systematic approach followed to build the CFD model yielded important information about the extent of the modelling uncertainties produced when different components of the CFD model were changed. Additionally, these results emphasize the need for a good rheological model selection and calibration for non-Newtonian fluids encountered in anaerobic digesters. Although a simple HB model was used to describe the rheological behaviour of Carbopol (similar to that of anaerobic sludge), the results showed that

the resulting fields were highly sensitive to the parameter values (especially in the laminar regime). To finalise, even if the use of mimicking fluids might not be entirely correct to fully describe the rheological behaviour of anaerobic sludges, these studies provide the first steps to identify the main sources of modelling errors for building future CFD models that will accurately describe the flow inside real digesters.

References

- Bugay, S., Escudie, R., Liné, A. (2002). *Experimental Analysis of Hydrodynamics in Axially Agitated Tank*, 48(3), 463–475.
- Chambon, G., Ghemmour, A., & Naaim, M. (2014). *Experimental investigation of viscoplastic free-surface flows in a steady uniform regime*. *Journal of Fluid Mechanics*, 754, 332–364.
- Fernandes del Pozo, D., Liné A., Van Geem K. M., Le Men, C., Nopens, I. (2019). *Hydrodynamic analysis of an axial impeller in a non-Newtonian fluid Through Particle Image Velocimetry*. In preparation.
- Eshtiaghi, N., Yap, S. D., Markis, F., Baudez, J. C., & Slatter, P. (2012). *Clear model fluids to emulate the rheological properties of thickened digested sludge*. *Water Research*, 46(9), 3014–3022.
- Lane, G. L. (2017). Improving the accuracy of CFD predictions of turbulence in a tank stirred by a hydrofoil impeller, 169, 188–211.
- Roberts, G., Barnes, H. *Rheol. Acta* (2001) 40: 499.
- Wicklein E., Batstone D. J., Ducoste J., Laurent J., Potier O., Nopens I. (2016). *Good Modelling practice in applying computational fluid dynamics for WWTP modelling*. *Water Science and*

T
e
c
h
n
o
l
o
g
y
,
9
6
9
-
9
8